Growing extremely thin bulklike metal film on a semiconductor surface: Monolayer Al(111) on Si(111)

Ying Jiang, Yong-Hyun Kim, S. B. Zhang, Philipp Ebert, Shenyuan Yang et al.

Citation: Appl. Phys. Lett. **91**, 181902 (2007); doi: 10.1063/1.2804010
View online: http://dx.doi.org/10.1063/1.2804010
View Table of Contents: http://apl.aip.org/resource/1/APPLAB/v91/i18
Published by the American Institute of Physics.

Growing extremely thin bulklike metal film on a semiconductor surface: Monolayer Al(111) on Si(111)

Ying Jiang
Institute of Physics, Chinese Academy of Sciences, Beijing 100080, China

Yong-Hyun Kim and S. B. Zhang
National Renewable Energy Laboratory, Golden, Colorado 80401, USA

Philipp Ebert
Institut für Festkörperforschung, Forschungszentrum Jülich, Jülich 52425, Germany

Shenyuan Yang, Zhe Tang, Kehui Wu,[a] and E. G. Wang
Institute of Physics, Chinese Academy of Sciences, Beijing 100080, China

(Received 7 September 2007; accepted 10 October 2007; published online 29 October 2007)

We report combined scanning tunneling microscopy, x-ray photoelectron emission spectroscopy, electron energy loss spectroscopy, and theoretical study of the growth of ultrathin Al film on the Si(111) substrate. We show that by (i) a modification of the substrate reconstruction with a $\sqrt{3} \times \sqrt{3}$ surface and (ii) a choice of materials with commensurate lattices, atomically flat film can be obtained even at the ultimate one monolayer limit, while maintaining a bulklike atomic structure. Detailed analysis shows that this monolayer Al(111)-1×1 film is electronically decoupled from the Si substrate, and it shows metallic characteristics. © *2007 American Institute of Physics*.
[DOI: 10.1063/1.2804010]

For quite some time, epitaxial growth of thin metal films on semiconductor surfaces has been at the forefront of surface research. From scientific point of view, such films can exhibit unexpected but, often, magnificent macroscopic quantum size effects,[1] such as superconductivity transition temperature oscillation and quantum catalysis, whose magnitude increases superlinearly with the decrease in film thickness (L),[2–6] limited by the roughness of the metal-semiconductor interface. From the practical point of view, the understanding of physicochemical properties of ultrathin metal films could promote the production and usage of clean and renewable energy, which may require the use of precious metals as catalyst in megascale.[7] Metal films are also elementary building blocks of microelectronic devices, as well as of the emerging magnetic data storage and subwavelength surface plasmonic devices.[8] With device miniaturization to the nanometer scale, their performance has also started to show clear reliance on the atomic level control of film morphology, thickness, and structure at the interface.

Semiconductor surfaces are often reconstructed, which disrupts the bulklike stacking at the surface. On such surfaces, metals usually form an initial disordered "wetting layer," followed, at room temperature, by the growth of three-dimensional islands with flat plateaus.[9–12] In contrast, by employing low temperature deposition and subsequent warming up to room temperature, smooth and continuous film can be formed above critical thicknesses of typically 4–7 ML.[2,4,6,10–12] However, besides the thickness limitation, this method also gives no control of the structure at the interface.

In this paper, we report the growth of a bulklike metal film on a semiconductor surface down to its ultimate limit: namely, an almost perfect monolayer thick Al(111)-1×1 film (denoted as Al-1×1) on Si(111)-1×1 substrate. Moreover, this monolayer Al-1×1 film is metallic, and electronically decoupled from the Si(111) substrate, such that its physical properties resemble those of a freestanding Al(111)-1×1 monolayer. Our findings are supported by first-principles electronic structure calculations.

The experiments were performed in an ultrahigh vacuum system (base pressure $<1 \times 10^{-10}$ mbar) equipped with scanning tunneling microscopy (STM), electron energy loss spectroscopy (EELS), x-ray photoelectron emission spectroscopy (XPS), and low energy electron diffraction (LEED). The Si(111)-$\sqrt{3} \times \sqrt{3}$-Al substrate was prepared by evaporating 1/3 ML Al atoms onto the Si(111)-7×7 surface at room temperature followed by annealing at 650 °C for 1 min, and the Al film was grown with the substrate cooled to 120 K and Al flux of 0.07 ML/min.

Al(111) on Si(111) is a so-called "magic mismatch" system[13] in that (1) both Al (111) and Si(111) have a hexagonal lattice with the lattice constants $a_{(\mathrm{Al})}=2.8630$ Å and $a_{(\mathrm{Si})}=3.840$ Å, respectively, and (2) because $2.863/3.84 (=0.745\,57) \approx 3/4 (=0.75)$, a 3×3 unit cell of Si(111)-1×1 will match very nicely with a 4×4 unit cell of Al(111)-1×1 with mismatch $<0.4\%$. Therefore, one may expect an epitaxial growth of Al(111) on Si(111) with negligible interfacial strain. Unfortunately, this is not observed: On Si(111)-7×7 substrates either islands (at room temperature) or a continuous film (>4 ML, at low temperature) are obtained, both, however, with rough interfaces.[14] Hence, to achieve good epitaxial growth, one must remove the 7×7 reconstruction to restore as close as possible the Si-1×1 surface.

For this purpose we adopt the Si(111)-$\sqrt{3} \times \sqrt{3}$-Al surface as the starting substrate. The Si(111)-$\sqrt{3} \times \sqrt{3}$-Al surface [Fig. 1(a)] consists of a bulk-terminated Si(111)-1×1 and 1/3 ML Al adatoms [with respect to the atomic density

[a]Author to whom correspondence should be addressed. Electronic mail: khwu@aphy.iphy.ac.cn

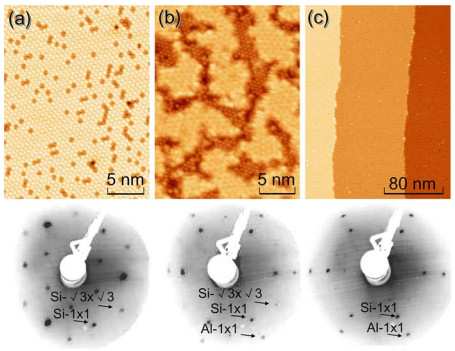

FIG. 1. (Color online) (a) Atomically resolved (empty state) STM image of the Si(111)-$\sqrt{3}\times\sqrt{3}$-Al surface. [(b) and (c)] 0.49 and 0.82 ML Al on the $\sqrt{3}\times\sqrt{3}$-Al surface, respectively. Steps in (c) arise from those in the original Si surface. Below the STM images are the corresponding LEED patterns.

of Si(111)]. Upon Al growth, two-dimensional (2D) Al islands form, as shown, for example, in Fig. 1(b) with 0.49 ML Al [from now on, 1 ML Al refers to the atomic density of Al(111) instead Si(111)]. At this stage, LEED shows simultaneously Si-1×1, Si-$\sqrt{3}\times\sqrt{3}$, and Al-1×1 patterns. While the Si-$\sqrt{3}\times\sqrt{3}$ pattern is from the uncovered $\sqrt{3}\times\sqrt{3}$ areas, the Al-1×1 pattern shows that the top surface of the 2D Al islands is a perfect Al(111)-1×1 layer. With increasing Al coverage, the 2D islands grow laterally until they form a perfectly smooth film, as shown in Fig. 1(c). The corresponding LEED shows a very sharp Al-1×1 pattern overlapping with the Si-1×1 pattern.

At a first glance, the 1×1-Al layer appears to form on top of the $\sqrt{3}\times\sqrt{3}$-Al surface preserving the $\sqrt{3}\times\sqrt{3}$-Al adatoms underneath. However, a careful Al coverage calibration shows that the Al-1×1 layer requires only 0.82 ML Al instead of 1 ML for completion.[15] The lack of 0.18 ML Al atoms may only be explained if the initial $\sqrt{3}\times\sqrt{3}$-Al adatoms ($\approx$0.19 ML) are also incorporated into the Al film during the growth, giving rise to a Al(111)-1×1 layer lying *directly* on top of the bulk-terminated Si(111)-1×1 substrate.

The model is further supported by the observation of a moiré pattern on the Al film surface [Fig. 2(a)]. The moiré pattern is hexagonal, in parallel with the lattice of the Si-1×1 substrate, with its periodicity (1.15 ± 0.10 nm) about

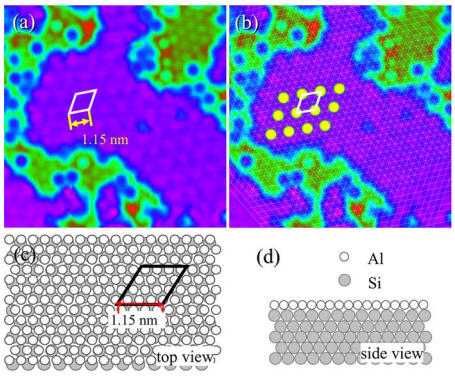

FIG. 2. (Color online) (a) STM image of a 12.5×12.5 nm^2 surface area where uncovered $\sqrt{3}\times\sqrt{3}$-Al substrate (green) coexists with 2D Al islands (purple). (b) Same as in (a) but the underlying position of the Si-1×1 lattice has been shown in a grid. Protrusions on the surface of Al islands are highlighted by yellow dots. (c) and (d) illustrate the structure model of Al-1×1 on top of Si-1×1.

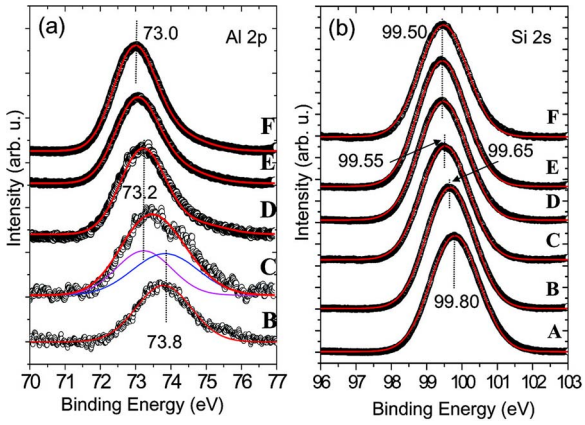

FIG. 3. (Color online) [(a) and (b)] XPS spectra of Al 2*p* and Si 2*p* peaks for surfaces with different Al coverages. (A) 7×7 without Al, (B) Si-$\sqrt{3}\times\sqrt{3}$-Al, (C) mixed $\sqrt{3}\times\sqrt{3}$-Al and Al-1×1, (D) Al-1×1, and [(E) and (F)] 1.5, and 4.3 additional ML Al, respectively, on (D). The spectra are fitted with Gaussian curves.

three times that of Si(111)-1×1. Such a moiré pattern can be generated if the Al(111)-1×1 lattice lies in parallel and directly on top of the Si(111)-1×1 lattice, as depicted in Figs. 2(c) and 2(d).

Further evidence of the above model is provided by *in situ* XPS measurements. Figure 3(a) shows the evolution of the Al 2*p* peak with the increasing Al coverage. Curves B, C, and D are recorded from the Si(111)-$\sqrt{3}\times\sqrt{3}$-Al substrate, half-ML Al-1×1 covered surface, and 1 ML Al-1×1 covered surface, respectively. In curve B, the binding energy (BE) of the Al 2*p* peak is 73.8 eV, about 0.8 eV blueshifted with respect to the bulk value of 73.0 eV. This shift is caused by the strong Al–Si bonds and charge transfer from Al to Si atoms on the $\sqrt{3}\times\sqrt{3}$-Al surface.[16] In curve D, the BE of the Al peak moves to 73.2 eV, quite close to the bulk value of 73.0 eV, indicating that, on average, the amount of charge loss per Al atom is already small. Note that the full width at half maximum of the Al 2*p* peak in both curve B and curve D is about 1.6 eV, indicating that they are both from a pure phase of Al. In contrast, for a mixed-phase surface such as in curve C, the Al 2*p* peak is significantly broadened and can be deconvolved into two peaks at 73.8 and 73.2 eV, respectively, corresponding nicely to the single-phase BEs in curve B and curve D. These results unambiguously confirm that a $\sqrt{3}\times\sqrt{3}$-Al layer does not exist underneath the Al(111)-1×1 film.

The corresponding Si 2*p* peaks are shown in Fig. 3(b). Curve A is recorded for the clean Si(111)-7×7 surface, whereas curves B–F are for the same surfaces depicted in Fig. 3(a). We observe a redshift of the Si 2*p* peak from 99.80 to 99.50 eV from curves A to D, which no longer changes with increasing Al coverage. The shift is toward red because Si receives charge from Al, instead. Again, the charge transfer effect vanishes soon after the completion of a fully covered Al-1×1 layer. The XPS results not only prove that the Al-1×1 layer lies directly on top of the Si-1×1 surface but also suggest that the Al-1×1 layer is electronically decoupled from the Si substrate, as the charge transfer becomes very weak upon the completion of a full Al monolayer.

It is of great interest why a $\sqrt{3}\times\sqrt{3}$-Al layer *cannot exist* underneath the Al-1×1 layer, but rather be incorporated into

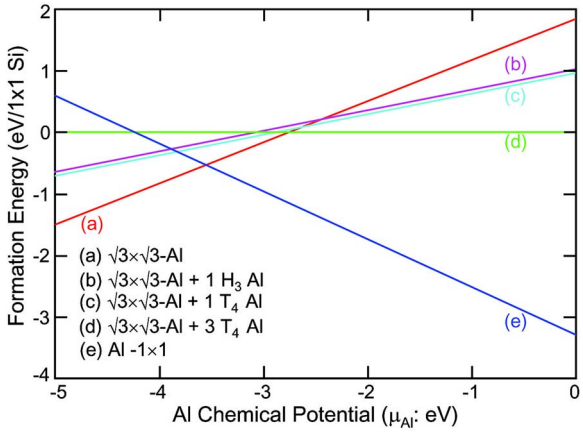

FIG. 4. (Color online) Calculated surface formation energy vs Al chemical potential (μ_{Al}) for the various Al structures on Si (111). The energies are all referenced to (d). The zero of μ_{Al} here corresponds to the formation of bulk Al, which sets the upper limit for μ_{Al}.

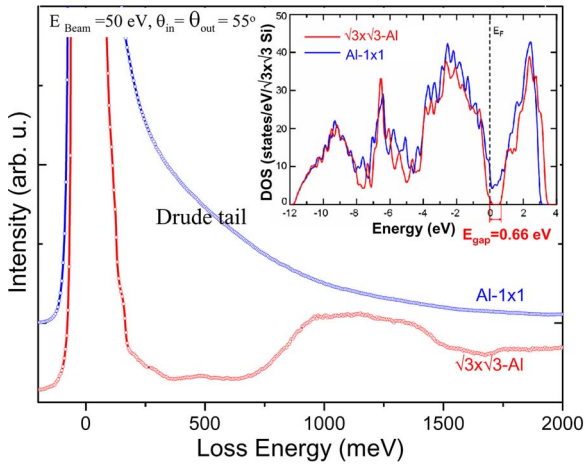

FIG. 5. (Color online) EELS spectra for the Si-$\sqrt{3}\times\sqrt{3}$-Al (red) and Al-1 $\times$1 (blue) surfaces. Inset: density of states calculated by DFT with 0.1 eV Gaussian broadening.

the layer. We calculated the formation energy of various Al adlayer structures on the Si(111) substrate as a function of the Al chemical potential μ_{Al} using the density functional theory (DFT).[17] On the $\sqrt{3}\times\sqrt{3}$-Al surface, Al adatoms are located at T_4 sites.[18] Starting from the $\sqrt{3}\times\sqrt{3}$-Al(T_4), the next Al adatom can be located either at H_3 or T_4 sites. Thus, we have five possible models: (a) $\sqrt{3}\times\sqrt{3}$-Al, (b) $\sqrt{3}\times\sqrt{3}$-Al+1H_3Al, (c) $\sqrt{3}\times\sqrt{3}$-Al+1T_4Al, (d) $\sqrt{3}\times\sqrt{3}$+3T_4Al, and (e) Al-1$\times$1, corresponding to 0.19, 0.38, 0.38, 0.56, and 1.0 ML Al coverages, respectively. Models (b) and (c) represent Al film growth with a $\sqrt{3}\times\sqrt{3}$-Al layer underneath, while models (d) and (e) represent Al growth without it.

Figure 4 shows that at low μ_{Al}, corresponding to Al poor, the $\sqrt{3}\times\sqrt{3}$-Al structure is the most stable one. As μ_{Al} increases, a crossover between the $\sqrt{3}\times\sqrt{3}$-Al and Al-1$\times$1 surfaces takes places. The Al-1$\times$1 surface remains to be the most stable surface for $-3.56\ \text{eV} < \mu_{Al} < 0$. Nowhere in the entire chemical potential range, the (b) $\sqrt{3}\times\sqrt{3}$-Al+1H_3Al and (c) $\sqrt{3}\times\sqrt{3}$-Al+1T_4Al surfaces are ever stable. Even the (d) $\sqrt{3}\times\sqrt{3}$+3T_4Al surface is unstable. This explains why in the intermediate Al coverage in Fig. 1(b), only the $\sqrt{3}\times\sqrt{3}$-Al and Al-1$\times$1 LEED spots are observed.

In order to verify the metallicity of the Al-1$\times$1 surface, we performed EELS measurement on the Al-1$\times$1 and $\sqrt{3}\times\sqrt{3}$-Al surfaces (Fig. 5). While the spectrum of the $\sqrt{3}\times\sqrt{3}$-Al shows a band gap, that of the Al-1$\times$1 layer shows a monotonic decaying continuum (Drude tail) completely filling the band gap region of the $\sqrt{3}\times\sqrt{3}$-Al surface. This shows that the monolayer Al-1$\times$1 film is indeed metallic, which is also supported by our first principles calculations (inset of Fig. 5).

In summary, we have demonstrated an extreme case of metals on semiconductor surfaces with abrupt interfaces, even down to the 1 monolayer limit. Key in our method is (1) the removal of the semiconductor surface reconstruction by a clever choice of "pseudo-1$\times$1" such as the Si(111)-$\sqrt{3}\times\sqrt{3}$-Al and (2) the use of a metal that satisfies the "magic mismatch" with the substrate. The film is not only structurally almost perfect, but it is also metallic, and electronically decoupled from the substrate to exhibit its own distinct physical properties.

This work at Beijing was supported by NSF of China (Contract No. 60021403) and CAS, and at NREL (Y.H.K. and S.B.Z.) was supported by the U.S. DOE/BES under Contract No. DE-AC36-99GO10337.

[1] F. K. Schulte, Surf. Sci. **55**, 427 (1976).
[2] M. Jalochowski, E. Bauer, H. Knoppe, and G. Lilienkamp, Phys. Rev. B **45**, 13607 (1992).
[3] Z. Zhang, Q. Niu, and C. K. Shih, Phys. Rev. Lett. **80**, 5381 (1998).
[4] Y. Guo, Y. F. Zhang, X. Y. Bao, T. Z. Han, Z. Tang, L. X. Zhang, W. G. Zhu, E. G. Wang, Q. Niu, Z. Q. Qiu, J. F. Jia, Z. X. Zhao, and Q. K. Xue, Science **306**, 1915 (2004).
[5] D. Eom, S. Qin, M. Y. Chou, and C. K. Shih, Phys. Rev. Lett. **96**, 027005 (2006).
[6] L. Aballe, A. Barinov, A. Locatelli, S. Heun, and M. Kiskinova, Phys. Rev. Lett. **93**, 196103 (2004).
[7] B. C. H. Steele, and A. Heinzel, Nature (London) **414**, 345 (2001).
[8] W. L. Barnes, A. Dereux, and T. W. Ebbesen, Nature (London) **424**, 824 (2003).
[9] A. J. Slavin, Prog. Surf. Sci. **50**, 159 (1995).
[10] A. R. Smith, K. J. Chao, Q. Niu, and C. K. Shih, Science **273**, 226 (1996).
[11] L. Gavioli, K. R. Kimberlin, M. C. Tringides, J. F. Wendelken, and Z. Zhang, Phys. Rev. Lett. **82**, 129 (1998).
[12] W. B. Su, S. H. Chang, W. B. Jian, C. S. Chang, L. J. Chen, and T. T. Tsong, Phys. Rev. Lett. **86**, 5116 (2001).
[13] A. Zur and T. C. McGill, J. Appl. Phys. **55**, 378 (1984).
[14] H. Liu, Y. F. Zhang, D. Y. Wang, M. H. Pan, J. F. Jia, and Q. K. Xue, Surf. Sci. **571**, 5 (2004).
[15] Y. Jiang, K. H. Wu, Z. Tang, P. Ebert, and E. G. Wang, Phys. Rev. B **76**, 035409 (2007).
[16] R. J. Hamers, Phys. Rev. B **40**, 1657 (1989).
[17] For the total energy calculation, we used the VASP codes with PAW potentials [G. Kresse and J. Joubert, Phys. Rev. B **59**, 1758 (1999)]. The energy cutoff for the wavefunction expansion was 300 eV, and the Perdew-Burke-Ernzerhof exchange-correlation functional [J. P. Perdew, K. Burke, and M. Ernzerhof, Phys. Rev. Lett. **77**, 3865 (1996)] was used. To study surfaces, we used a slab with eight Si(111) double layers and a vacuum of 15 Å thickness. For the Brillouin-zone integration, we used the (12$\times$12$\times$1), (8$\times$8$\times$1), and (4$\times$4$\times$1) k-point sets in the $M-P$ scheme [H. J. Monkhorst and J. D. Pack, Phys. Rev. B **13**, 5188 (1976)] for Si 1$\times$1, $\sqrt{3}\times\sqrt{3}$, and Al-1$\times$1 surfaces, respectively.
[18] J. E. Northrup, Phys. Rev. Lett. **53**, 683 (1984).